

Neutrino emission from a GRB afterglow shock during an inner supernova shock breakout

Y.W. Yu^{1,2*}, Z.G. Dai^{1†}, and X.P. Zheng^{2‡}

¹*Department of Astronomy, Nanjing University, Nanjing 210093, China*

²*Institute of Astrophysics, Huazhong Normal University, Wuhan 430079, China*

21 November 2018

ABSTRACT

The observations of a nearby low-luminosity gamma-ray burst (GRB) 060218 associated with supernova SN 2006aj may imply an interesting astronomical picture where a supernova shock breakout locates behind a relativistic GRB jet. Based on this picture, we study neutrino emission for early afterglows of GRB 060218-like GRBs, where neutrinos are expected to be produced from photopion interactions in a GRB blast wave that propagates into a dense wind. Relativistic protons for the interactions are accelerated by an external shock, while target photons are basically provided by the incoming thermal emission from the shock breakout and its inverse-Compton scattered component. Because of a high estimated event rate of low-luminosity GRBs, we would have more opportunities to detect afterglow neutrinos from a single nearby GRB event of this type by IceCube. Such a possible detection could provide evidence for the picture described above.

Key words: gamma rays: bursts — elementary particles

1 INTRODUCTION

Gamma-ray burst (GRB) 060218 associated with SN 2006aj discovered by Swift (Campana et al. 2006) provides a new example of low-luminosity GRBs (LL-GRBs), as its isotropic equivalent energy ($\sim 6 \times 10^{49}$ erg) is 100 to 1000 times less but its duration ($T_{90} = 2100 \pm 100$ s) is much longer than those of conventional high-luminosity GRBs. More interestingly, besides an usual non-thermal component in its early X-ray spectrum, a surprising thermal component was observed by the Swift XRT during both burst and afterglow phases. Fitting with a blackbody spectrum, the temperature of this thermal component was inferred to be $kT \sim 0.17$ keV during the first 3 ks. When $t > 10$ ks, however, the peak energy of the blackbody decreased and then passed through the Swift UVOT energy range at ~ 100 ks (Campana et al. 2006; Blustin 2007).

To explain the prompt emission, in principle, a model based on the internal dissipation of relativistic ejecta may be valid in the case of GRB 060218. The relativistic GRB ejecta, which interacts with a dense wind surrounding the progenitor, has also been required to understand a power-law decaying afterglow in X-ray and radio bands about ~ 10 ks after the burst, although some complications beyond the

standard afterglow model are involved (Soderberg et al. 2006; Fan et al. 2006; Waxman et al. 2007). Furthermore, as suggested by Wang & Mészáros (2006), the soft X-ray thermal emission could arise from a shock breakout, namely, a hot cocoon that breaks out from the supernova ejecta and the stellar wind. In detail, a more rapid part of a jet moving in the envelope and the dense wind is accelerated to a highly-relativistic velocity to produce the GRB, while a slower part of the jet together with the outermost parts of the envelope becomes a mildly relativistic cocoon (Mészáros & Rees 2001; Ramirez-Ruiz et al. 2002; Zhang et al. 2003), which locates behind the GRB blast wave.

Although the GRB blast wave runs in front of the shock breakout, the thermal emission from the latter outshines the former persistently until the emission of the breakout is switched off. Thus, the emission properties of the GRB blast wave (consisting of external shock-accelerated electrons and protons) should be influenced by the incoming thermal photons significantly during both burst and early afterglow phases. On one hand, the cooling of the relativistic electrons, which upscatter the thermal photons, could be dominated by inverse-Compton (IC) radiation rather than synchrotron radiation (Wang & Mészáros 2006). On the other hand, inferred from the observations, the intensity of the thermal emission could be comparable in the same band to the one of the prompt emission due to internal dissipations and much larger than the one of the afterglow emission due to an external shock. Therefore, the thermal photons as

* yuyw@nju.edu.cn (YWY)

† dzg@nju.edu.cn (ZGD)

‡ zhxp@phy.cnu.edu.cn (XPZ)

target photons for photopion interactions could also play an important role in the energy loss of the relativistic protons and thus influence or even dominate neutrino emission of the GRB blast wave.

It has been widely studied that conventional GRBs in the standard internal-external shock model emit high energy neutrinos during the burst, early afterglow, and X-ray flare phases (Waxman & Bahcall 1997, 2000; Dai & Lu 2001; Dermer 2002; Dermer & Atoyan 2003; Asano 2005; Murase & Nagataki 2006a, 2006b; Murase 2007; Gupta & Zhang 2007). In contrast to the conventional GRBs, LL-GRBs may have a much higher event rate (several hundred to thousand events $\text{Gpc}^{-3}\text{yr}^{-1}$), which is inferred from the fact that two typical nearby LL-GRBs, i.e., GRB 060218 and GRB 980425, have been observed within a relatively short period of time (Cobb et al. 2006; Soderberg 2006; Liang et al. 2007). The high event rate implies that the contribution from LL-GRBs to the diffuse neutrino background may be important and that we have more opportunities to detect neutrinos from a very nearby single LL-GRB event. Therefore, Murase et al. (2006) and Gupta & Zhang (2006) recently studied the neutrino emission properties of LL-GRBs during their burst phase using the internal shock model, in which the target photons for photopion interactions are mainly provided by internal shock-driven non-thermal emission. In this paper, however, we will focus on the early afterglow neutrino emission. During this phase, relativistic protons are accelerated by an external shock (rather than internal shocks) and target photons are dominated by the incoming thermal emission and even its IC scattered component.

This paper is organized as follows. In section 2 we briefly describe the dynamics of a GRB blast wave propagating into a surrounding dense wind. In section 3, we give the photon distribution in the blast wave by considering the incoming thermal emission and its IC scattered component, but the weak synchrotron radiation of the electrons is ignored. In section 4, neutrino spectra are derived formally with an energy loss timescale of protons due to photopion interactions. In section 5, we calculate the timescale and then the neutrino spectra using the target photon spectra obtained in section 3 and an experiential fitting formula of the cross section of photopion interactions. In addition, the peak of a neutrino spectrum is also estimated analytically by using Δ -approximation. Finally, a summary is given in section 6.

2 DYNAMICS OF A GRB BLAST WAVE

We consider a GRB jet with isotropic equivalent energy $E = 10^{50} E_{50}$ erg (hereafter $Q_x = Q/10^x$) expanding into a dense wind medium with density profile $\rho(r) = Ar^{-2}$. Here, the coefficient A is determined by the mass loss rate and velocity of the wind of the progenitor, i.e., $A = \dot{M}/4\pi v_w = 5.0 \times 10^{11} \text{g cm}^{-1} A_*$, where $A_* \equiv [\dot{M}/(10^{-5} M_\odot \text{yr}^{-1})][v_w/(10^3 \text{km s}^{-1})]^{-1}$. From Dai & Lu (1998) and Chevalier & Li (2000), we get the Lorentz factor and radius of the GRB blast wave (i.e., the external-shocked wind gas) respectively as

$$\Gamma = \left(\frac{9E}{128\pi Ac^3 t} \right)^{1/4} = 3.6 E_{50}^{1/4} A_*^{-1/4} t_3^{-1/4}, \quad (1)$$

$$r = \left(\frac{9Et}{2\pi Ac} \right)^{1/2} = 3.1 \times 10^{15} \text{cm} E_{50}^{1/2} A_*^{-1/2} t_3^{1/2}. \quad (2)$$

They satisfy $r = 8\Gamma^2 ct$, which gives rise to a relationship, $t' = (16/3)\Gamma t$, between the dynamic time t' measured in the rest frame of the blast wave and the observed time t (Dai & Lu 1998).

As the circum-burst wind materials are swept up and shocked, most of the heated electrons before cooling concentrate at the minimum Lorentz factor $\gamma'_{e,m} \sim \bar{\epsilon}_e \frac{m_p}{m_e} \Gamma = 659 \bar{\epsilon}_{e,-1} E_{50}^{1/4} A_*^{-1/4} t_3^{-1/4}$. The symbol $\bar{\epsilon}_e \equiv \epsilon_e(p-2)/(p-1)$, where ϵ_e is the usual equipartition factor of the hot electrons and p is the electron's energy distribution index (where $p > 2$ is only considered). Meanwhile, a fraction ϵ_B of the internal energy is assumed to be occupied by a magnetic field, and then the strength of the magnetic field is calculated by $B' \sim (32\pi\epsilon_B\Gamma^2\rho c^2)^{1/2} = 78\text{G} \epsilon_{B,-1}^{1/2} E_{50}^{-1/4} A_*^{3/4} t_3^{-3/4}$. Finally, the other energy (a fraction of $\epsilon_p = 1 - \epsilon_e - \epsilon_B$) is carried by the accelerated protons. For these protons, we can estimate their maximum energy by $E_{p,\text{max}} = 2eB'r/3 = 4.8 \times 10^{10} \text{GeV} \epsilon_{B,-1}^{1/2} E_{50}^{1/4} A_*^{1/4} t_3^{-1/4}$ by equating the acceleration time to the shorter of the dynamic time and the synchrotron cooling time (Razzaque et al. 2006). However, the minimum energy of the protons is unknown, but the corresponding Lorentz factor $\gamma'_{p,\text{min}}$ is thought to be close to $\sim \Gamma$.

3 PHOTON EMISSION

The photons in the GRB blast wave have two origins, i.e., the blast wave self and the inner supernova shock breakout. The electrons in the blast wave emit photons via synchrotron and IC scattering processes. Moreover, as analyzed by Wang & Mészáros (2006), the synchrotron radiation (peaking within X-ray band) of the blast wave electrons is inferred from the observations to be much weaker than the incoming thermal emission, and thus the cooling of the electrons should be dominated by their IC scattering off the thermal photons. Therefore, in following calculations, we consider the thermal emission and its subsequent IC scattered component only.

The properties of the supernova shock breakout have been unclear to date. We suppose that it has a constant blackbody temperature of $kT = 0.1\text{keV}(kT)_{-1}$ and a constant radius of the emission region of $R = 10^{12} \text{cm} R_{12}$. The lifetime t_{SB} of this high-temperature emission is about thousands of seconds, which is considered to be several to several ten times longer than the duration of the GRB. Then, the isotropic equivalent luminosity and energy of the shock breakout can be estimated by $L_{\text{SB}} = 4\pi R^2 \sigma T^4 = 1.3 \times 10^{45} \text{erg s}^{-1} (kT)_{-1}^4 R_{12}^2$ and $E_{\text{SB}} = 1.3 \times 10^{48} \text{erg} (kT)_{-1}^4 R_{12}^2 t_{\text{SB},3}$, respectively. Meanwhile, it is easy to write the monochromatic number density of these thermal photons at the breakout as

$$n(E_\gamma) = \frac{8\pi}{h^3 c^3} \frac{E_\gamma^2}{\exp(E_\gamma/kT) - 1} = \frac{8\pi k^2 T^2}{h^3 c^3} \phi\left(\frac{E_\gamma}{kT}\right), \quad (3)$$

where the function $\phi(x) = x^2/(e^x - 1)$. Assuming that the photons propagate freely before they reach the GRB blast wave at radius r , we can calculate the density of the thermal photons in the blast wave by multiplying a factor $(R/r)^2$ to Eq. (3). Subsequently, after Lorentz transformation, we

obtain the density of the incoming photons in the blast wave measured in its rest frame by

$$n'_{\text{in}}(E'_{\gamma,\text{in}}) = \frac{R^2}{r^2} n(\Gamma E'_{\gamma,\text{in}}) = \frac{R^2}{r^2} \frac{8\pi k^2 T^2}{h^3 c^3} \phi\left(\frac{3E'_{\gamma,\text{in}}}{E'_{\gamma,\text{pk1}}}\right), \quad (4)$$

where $E'_{\gamma,\text{pk1}} \equiv 3kT/\Gamma$ is the peak energy of the black body spectrum. When these photons cross the blast wave, a part of them should be upscattered by the relativistic electrons. The energy of the IC scattered photons can be estimated by $E'_{\gamma,\text{IC}} = 2\gamma'^2_{e,m} E'_{\gamma,\text{in}}$ and the corresponding density by

$$\begin{aligned} n'_{\text{IC}}(E'_{\gamma,\text{IC}}) &= \frac{\tau}{2\gamma'^2_{e,m}} n'_{\text{in}}\left(\frac{E'_{\gamma,\text{IC}}}{2\gamma'^2_{e,m}}\right) \\ &= \frac{\tau}{2\gamma'^2_{e,m}} \frac{R^2}{r^2} \frac{8\pi k^2 T^2}{h^3 c^3} \phi\left(\frac{3E'_{\gamma,\text{IC}}}{E'_{\gamma,\text{pk2}}}\right), \end{aligned} \quad (5)$$

where $E'_{\gamma,\text{pk2}} \equiv 6\gamma'^2_{e,m} kT/\Gamma$. The probability of the scattering is represented by the photon optical depth of the blast wave, $\tau = \sigma_{\text{T}}(A/m_p r) = 6.5 \times 10^{-5} E_{50}^{-1/2} A_*^{3/2} t_3^{-1/2}$, where σ_{T} is the Thomson cross section. According to this estimation, Wang & Mészáros (2006) predicted that the early afterglow spectra of GRB 060218-like GRBs may have a bimodal profile peaking at

$$E_{\gamma,\text{pk1}} = 0.3 \text{ keV } (kT)_{-1} \quad (6)$$

and

$$E_{\gamma,\text{pk2}} = 0.26 \text{ GeV } \tilde{\epsilon}_{e,-1}^2 (kT)_{-1} E_{50}^{1/2} A_*^{-1/2} t_3^{-1/2}. \quad (7)$$

Thus, a significant sub-GeV or GeV emission component accompanying the thermal emission would be detectable with the upcoming *Gamma-ray Large Area Space Telescope*, which could provide evidence for the GRB jet.

4 NEUTRINO PRODUCTION

Since relativistic protons in the GRB blast wave are immersed in the photon field described above, the protons would lose their energy to produce mesons such as π^0 and π^\pm etc, and subsequently generate neutrinos by the decay of π^\pm , i.e., $\pi^\pm \rightarrow \mu^\pm + \nu_\mu(\bar{\nu}_\mu) \rightarrow e^\pm + \nu_e(\bar{\nu}_e) + \bar{\nu}_\mu + \nu_\mu$. During these processes, the energy loss rate of a proton with energy $E'_p = \gamma'_p m_p c^2$ can be calculated by (Waxman & Bahcall 1997)¹

$$\begin{aligned} t'^{-1}_\pi &\equiv -\frac{1}{E'_p} \frac{dE'_p}{dt'} \\ &= \frac{c}{2\gamma'^2_p} \int_{\tilde{E}_{\text{th}}}^{\infty} \sigma_\pi(\tilde{E}) \xi(\tilde{E}) \tilde{E} \\ &\quad \times \left[\int_{\tilde{E}/2\gamma'_p}^{\infty} n'(E'_\gamma) E'^{-2}_\gamma dE'_\gamma \right] d\tilde{E}, \end{aligned} \quad (8)$$

where $\sigma_\pi(\tilde{E})$ is the cross section of photopion interactions for a target photon with energy \tilde{E} in the proton's rest frame,

¹ To obtain this expression, an isotropic target photon field is required. However, in our model, the radially incoming photon field is seen by the protons in the blast wave anisotropically. This gives an extra complication for a more realistic consideration. For simplicity, we ignore the anisotropic effect in our calculations.

ξ is the inelasticity defined as the fraction of energy loss of a proton to the resultant pions, and $\tilde{E}_{\text{th}} = 0.15 \text{ GeV}$ is the threshold energy of the interactions. Equation (8) yields that the energy of the protons decreases as $\exp\left[-\int_0^{t'} (dt'/t'_\pi)\right]$. In our scenario, if the shock-breakout emission could last for a period of t_{SB} , the fraction of the energy loss of the protons to pions could be calculated by

$$f_\pi = 1 - \exp\left(-\int_0^{t'_{\text{SB}}} \frac{dt'}{t'_\pi}\right), \quad (9)$$

where $t'_{\text{SB}} = (16/3)\Gamma t_{\text{SB}}$. In order to calculate t'_π , the crucial input in the model is the target photon spectrum $n'(E'_\gamma)$. From Eqs. (4) and (5), we know that $n'(E'_\gamma)$ depends on both r and Γ and thus the value of t'_π could evolve with time. However, if t'_π is independent of time or varies with time slowly, Eq. (9) can be also approximated by

$$f_\pi \approx 1 - \exp(-t'_{\text{SB}}/t'_\pi) \approx \min[t'_{\text{SB}}/t'_\pi, 1] \quad (10)$$

as usual, especially for analytical calculations.

To be specific, the energy loss of the protons is shared by π^\pm and π^0 with a certain ratio. Unfortunately, it is not easy to fix this ratio due to the complications arising from various single-pion and multipion production processes. In following calculations, we simply take it to be a constant, $\pi^\pm : \pi^0 = 2 : 1$, as in Asano (2005). Furthermore, two resultant muon-neutrinos from the decay of a π^\pm could inherit half of the pion's energy roughly evenly. Therefore, we can relate the neutrino energy E_ν to the energy loss of the primary proton by

$$E_\nu = \frac{1}{4} \xi E_p, \quad (11)$$

and give an observed time-integrated muon-neutrino spectrum by

$$E_\nu^2 \phi_\nu \equiv \frac{1}{4\pi D_l^2} E_p^2 \frac{dN_\nu}{dE_\nu} = \frac{1}{4\pi D_l^2} \frac{f_\pi}{3} E_p^2 \frac{dN_p}{dE_p}, \quad (12)$$

where D_l is the luminosity distance of the burst. As usual, we assume the energy distribution of the shock-accelerated protons to be $(dN_p/dE_p) \propto E_p^{-2}$, where the proportional coefficient can be calculated by $\epsilon_p E / \ln(E_{p,\text{max}}/E_{p,\text{min}})$.

In addition, because of the presence of the magnetic field, the ultrahigh energy pions and muons would lose their energy via synchrotron radiation before decay. This leads to breaks in the neutrino spectrum at (Murase 2007)

$$\begin{aligned} E_{\nu,\text{b}}^{s\pi} &= \frac{1}{4} E_{\pi,\text{b}} = \frac{1}{4} \Gamma \left(\frac{6\pi m_\pi^5 c^5}{\sigma_{\text{T}} m_e^2 B'^2 \tau_\pi} \right)^{1/2} \\ &= 1.2 \times 10^9 \text{ GeV } \epsilon_{B,-1}^{-1/2} E_{50}^{1/2} A_*^{-1} t_3^{1/2}, \end{aligned} \quad (13)$$

$$\begin{aligned} E_{\nu,\text{b}}^{s\mu} &= \frac{1}{3} E_{\mu,\text{b}} = \frac{1}{3} \Gamma \left(\frac{6\pi m_\mu^5 c^5}{\sigma_{\text{T}} m_e^2 B'^2 \tau_\mu} \right)^{1/2} \\ &= 8.9 \times 10^7 \text{ GeV } \epsilon_{B,-1}^{-1/2} E_{50}^{1/2} A_*^{-1} t_3^{1/2}, \end{aligned} \quad (14)$$

where $\tau_\pi = 2.6 \times 10^{-8} \text{ s}$ and $\tau_\mu = 2.2 \times 10^{-6} \text{ s}$ are the mean lifetimes of pions and muons in their rest frames. Above $E_{\nu,\text{b}}^s$, the neutrino flux would be suppressed by a factor $(E_\nu/E_{\nu,\text{b}}^s)^{-2}$ (Rachen & Mészáros 1998; Razzaque et al. 2006). However, as pointed out by Asano & Nagataki (2006), neutral kaons can survive in the magnetic field, while

the ultrahigh-energy charged pions and muons cool rapidly. Moreover, because kaons have a larger rest mass than pions and muons, charged kaons can reach higher energy although they also suffer from synchrotron cooling. Thus, decay of kaons, which is not taken into account in our calculations, may dominate neutrino emission above $\sim 10^8 - 10^9$ GeV.

Now, by inserting Eqs. (4) and (5) into Eq. (8) and then into Eq. (9) to get f_π , we can easily obtain the observed neutrino spectra from Eq. (12) for our scenario. The remaining task is only to express the cross section $\sigma_\pi(\tilde{E})$ and inelasticity for photopion interactions.

5 RESULTS

Since the cross section of photopion interactions peaks at $\tilde{E}_\Delta \simeq 0.3$ GeV due to the $\Delta(1232)$ -resonance, the integration over \tilde{E} in Eq. (8) can be roughly approximated by

$$t'_\pi{}^{-1} \approx \frac{c}{2\gamma_p'^2} \sigma_{\pi,\Delta} \xi_\Delta \tilde{E}_\Delta \delta \tilde{E} \int_{\tilde{E}_\Delta/2\gamma_p'}^{\infty} n'(E'_\gamma) E'^{-2}_\gamma dE'_\gamma, \quad (15)$$

where $\sigma_{\pi,\Delta} \approx 0.5$ mbarn, $\xi_\Delta \approx 0.2$, and the peak width is about $\delta \tilde{E} \approx 0.2$ GeV. Inserting Eq. (4) or (5) into Eq. (15), we use the approximative formula $f_\pi = \min[t'_{\text{SB}}/t'_\pi, 1]$ to obtain

$$f_\pi = \min \left\{ \frac{16}{3} \varsigma \frac{R^2}{r^2} \frac{8\pi k^2 T^2}{h^3 c^2} \frac{2E'_{\gamma,\text{pk}}}{3\tilde{E}_\Delta} \sigma_{\pi,\Delta} \xi_\Delta \delta \tilde{E} \Gamma t_{\text{SB}}, \right. \\ \left. \times \varepsilon_*^2 [\varepsilon_* - \ln(e^{\varepsilon_*} - 1)], 1 \right\}. \quad (16)$$

where $\varsigma = 1$ and $\tau/(2\gamma_{e,m}'^2)$ for pre- and post-upscattered target photons, respectively. The dimensionless variable ε_* is defined by $\varepsilon_* \equiv 3\tilde{E}_\Delta/(2\gamma_p' E'_{\gamma,\text{pk}}) = 3\xi_\Delta \Gamma^2 \tilde{E}_\Delta m_p c^2 / (8E_\nu E_{\gamma,\text{pk}})$. In the case of $f_\pi < 1$, the peak value of f_π reading

$$f_{\pi,\text{pk}} = 3\varsigma \frac{R^2}{r^2} \frac{8\pi k^2 T^2}{h^3 c^2} \frac{2E'_{\gamma,\text{pk}}}{3\tilde{E}_\Delta} \sigma_{\pi,\Delta} \xi_\Delta \delta \tilde{E} \Gamma t_{\text{SB}} \quad (17)$$

is at $\varepsilon_* = 1.8$, which gives rise to the relationship between the peak energies of the neutrino and photon spectra as $E_{\nu,\text{pk}} E_{\gamma,\text{pk}} = 0.01 \Gamma^2 \text{GeV}^2$. Considering the bimodal distribution of the target photons peaking at $E_{\gamma,\text{pk}1}$ and $E_{\gamma,\text{pk}2}$, two peaks are also expected in the resultant neutrino spectrum but only the one determined by $E_{\gamma,\text{pk}1}$ could fall into the high energy range ($E_\nu > \text{TeV}$) of our interest at

$$E_{\nu,\text{pk}} = 4.9 \times 10^5 \text{GeV} (kT)_{-1}^{-1} E_{50}^{1/2} A_*^{-1/2} t_{\text{SB},3}^{-1/2}. \quad (18)$$

In other words, the target photons for photopion interactions of interest are contributed by the incoming thermal emission mainly. The value of the differential neutrino fluence at $E_{\nu,\text{pk}}$ reads

$$[E_\nu^2 \phi_\nu]_{\text{pk}} = 2.0 \times 10^{-6} \text{erg cm}^{-2} \epsilon_p (kT)_{-1}^3 R_{12}^2 A_* D_{l,25.5}^{-2}, \quad (19)$$

which is calculated by using the peak value of f_π as

$$f_{\pi,\text{pk}} = 0.02 (kT)_{-1}^3 R_{12}^2 E_{50}^{-1} A_*. \quad (20)$$

On the other hand, when $f_\pi = 1$, $E_\nu^2 \phi_\nu$ would reach an upper limit as $1.2 \times 10^{-4} \text{erg cm}^{-2} \epsilon_p E_{50} D_{l,25.5}^{-2}$, which is determined by the total energy carried by the protons in the GRB blast wave.

Although it is convenient and effective to use the Δ -approximation to estimate the peak of a neutrino spectrum, the Δ -approximation would lead to a remarkable underestimation of the neutrino flux above the peak energy due to the non-zero cross section of photopion interactions in high energy regions. So, for more careful calculations, we provide an experiential fitting formula for the cross section as shown in Eq. (A5), which is extrapolated from experimental data taken from particle data group (Yao et al. 2006). However, since we can not find a simple expression for the inelasticity, we take $\xi = 0.2$ for all energy regions roughly, which may leads to a mild underestimation of the neutrino flux in the high energy regions. Finally, with these inputs, we plot the observed time-integrated muon-neutrino spectra in Fig. 1. Obviously, two plateaus exist in the neutrino spectra. To be specific, as shown in the upper panel of Fig.1, the high-energy plateau is produced by the lower energy thermal photons, while the low-energy plateau is produced by the higher energy IC scattered photons. In addition, from a comparison shown in the lower panel of Fig. 1, we can see that the approximation for f_π in Eq. (10) is feasible to some extent for the thermal seed photon-dominated photopion interactions, but not for the IC scattered photon-dominated interactions. This difference of these two kinds of interaction arises from different temporal behaviors of t'_π .

Next let's discuss the detectability of the afterglow neutrinos, using the following fitting formula for the probability of detecting muon-neutrinos by IceCube (Ioka et al. 2005; Razzaque et al. 2004)

$$P_\nu = 7 \times 10^{-5} \left(\frac{E_\nu}{3.2 \times 10^4 \text{GeV}} \right)^\beta, \quad (21)$$

where $\beta = 1.35$ for $E_\nu < 3.2 \times 10^4 \text{GeV}$, while $\beta = 0.55$ for $E_\nu \geq 3.2 \times 10^4 \text{GeV}$. The number of muon events from muon-neutrinos above TeV energy is given by

$$N_\mu = A_{\text{det}} \int_{\text{TeV}} \phi_\nu P_\nu dE_\nu, \quad (22)$$

where $A_{\text{det}} \sim 1 \text{km}^2$ is the geometrical detector area. Inserting Eqs. (12) and (21) into the above integral, we obtain $N_\mu \sim 0.1$ for the parameter set ($E_{50} = 1$, $A_* = 10$, $(kT)_{-1} = 2$, $R_{12} = 1$ and $t_{\text{SB},3} = 3$) inferred from GRB 060218 for a very nearby LL-GRB at 50 Mpc, where a LL-GRB event is expected to be observed within a many-years observation. According to this estimation, we expect optimistically that IceCube may be able to detect afterglow neutrinos from one LL-GRB event in the following decades. If such a detection comes true, the afterglow neutrino emission accompanying the soft X-ray thermal and sub-GeV or GeV emissions from a GRB 060218-like GRB event would provide strong evidence for the picture that a supernova shock breakout locates behind a relativistic GRB jet, and further would be used to constrain the model parameters severely.

Besides the possible detection of neutrinos from a single LL-GRB event, the contribution to the neutrino background from LL-GRBs is also expected to be important. We can estimate the diffuse muon-neutrino flux arising from afterglow neutrino emission of LL-GRBs by (Waxman & Bahcall 1998; Murase et al. 2006)

$$E_\nu^2 \Phi_\nu \sim \frac{c}{4\pi H_0} \frac{f_\pi}{3} f_b \epsilon_p E_p^2 \frac{dN_p}{dE_p} R_{\text{LL}}(0) f_z$$

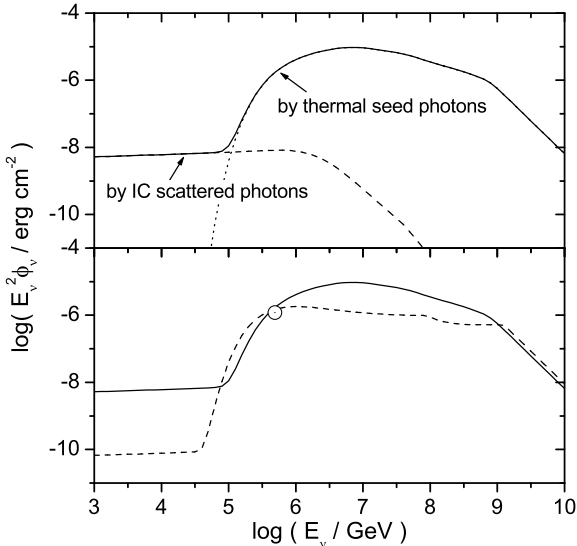


Figure 1. The time-integrated afterglow muon-neutrino ($\nu_\mu + \bar{\nu}_\mu$) spectra for one GRB event. The solid lines are calculated by using the expressions for f_π in Eq. (9) and for $\sigma_\pi(\tilde{E})$ in Eq. (A5). *Upper panel:* The contributions to the total neutrino emission by the two target photon components are represented by the dashed and dotted lines, respectively. *Lower panel:* The dashed line is obtained by an approximation for the time integration as in Eq. (10), and the peak estimated by the Δ -approximation is labeled by an open circle. In all cases, we take the model parameters E_{50} , A_* , $(kT)_{-1}$, R_{12} , $D_{l,25.5}$ and $t_{\text{SB},3}$ to be unity and the equipartition factors $\epsilon_e = 0.3$, $\epsilon_B = 0.1$ and thus $\epsilon_p = 0.6$.

$$= 2.5 \times 10^{-11} \text{GeV cm}^{-2} \text{s}^{-1} \text{sr}^{-1} \epsilon_p (kT)_{-1}^3 R_{12}^2 A_* \times f_b \left(\frac{R_{\text{LL}}(0)}{500 \text{Gpc}^{-3} \text{yr}^{-1}} \right) \left(\frac{f_z}{3} \right), \quad (23)$$

where $H_0 = 71 \text{km s}^{-1} \text{Mpc}^{-1}$, f_b is the beaming factor, and f_z is the correction factor for the possible contribution from high-redshift sources. In the above estimation, the approximate value of f_π in Eq. (20) is applied. By comparing Eq. (23) to Eq. (3) of Murase et al. (2006), we find that, for LL-GRBs, the contribution to the diffuse neutrino background by the early afterglow neutrino emission may be relatively smaller than or even comparable to (e.g., for model parameters $\epsilon_p = 0.6$, $(kT)_{-1} = 2$, $R_{12} = 1$, and $A_* = 10$) that by the burst neutrino emission.

Finally, we would like to refer the reader to neutrino oscillation, which will change neutrino flavor ratio from $\nu_e : \nu_\mu : \nu_\tau \simeq 1 : 2 : 0$ at the source to $1 : 1 : 1$ at the earth. This thus leads to the fact that the observed muon-neutrino fluxes estimated above should be reduced further by a factor of ~ 2 .

6 SUMMARY

The surprising soft X-ray thermal emission during both burst and afterglow phases of GRB 060218/SN 2006aj was proposed to be due to the breakout from a strong stellar wind of a radiation-dominated shock. This shock breakout was further thought to locate behind a relativistic GRB

jet, which is required by understanding the burst emission and the power-law decaying afterglow emission. Wang & Mészáros (2006) suggested that a sub-GeV or GeV emission produced by IC scattering of the thermal photons by the relativistic electrons in the GRB blast wave could give evidence for this astronomical picture. In this paper, we studied another possible implication, namely, afterglow neutrino emission. The neutrinos are produced by photopion interactions of relativistic protons, which could be accelerated by a relativistic external shock. The target photons in the interactions are contributed by the incoming thermal emission and its upscattered component. By considering the high event rate of LL-GRBs, we argue optimistically that the afterglow neutrinos from very nearby (several tens of Mpc) LL-GRBs may be detected by IceCube in the following decades. We believe the detection of these expected afterglow neutrinos is helpful to uncover the nature of GRB 060218-like GRBs.

ACKNOWLEDGEMENTS

We would like to thank the referee for helpful comments and suggestions. This work is supported by the National Natural Science Foundation of China (grants 10221001 and 10640420144) and the National Basic Research Program of China (973 program) No. 2007CB815404. Y.W.Y. is also supported by the Visiting PhD Candidate Foundation of Nanjing University and partly by the National Natural Science Foundation of China (grants 10603002 and 10773004).

APPENDIX A: CROSS SECTION FITS

The fits to the total cross section for $p\gamma$ interactions have been widely studied (e.g., Rachen 1996; Mücke et al. 2000). In physics, this cross section is contributed by resonant excitations and direct (non-resonant) single-pion production processes in the resonant energy regions and by statistical multipion production processes mainly and diffractive scattering slightly in the high energy region ($\tilde{E}_0 > 0.727 \text{ GeV}$).

It is known that the cross section for a resonance is given by the Breit-Wigner formula (Mücke et al. 2000)

$$\sigma_R(\tilde{E}) = \frac{s}{\tilde{E}^2} \frac{\sigma_0 \bar{\Gamma}^2 s}{(s - m_R^2 c^4)^2 + \bar{\Gamma}^2 s}, \quad (\text{A1})$$

where $\sqrt{s} = (m_p^2 c^4 + 2m_p c^2 \tilde{E})^{1/2}$ is the total energy of the colliding photon and proton in the mass-center frame, and m_R and $\bar{\Gamma}$ are the nominal mass and width of the resonance, respectively. The coefficient σ_0 is determined by the resonance angular momentum and the electromagnetic excitation strength. For nine important resonances in $p\gamma$ interactions, we take the related parameters from Mücke et al. (2000) and list them in Table 1. Then, the total cross section contributed by these resonances can be written as

$$\sigma_1(\tilde{E}) = \left[1 - \exp\left(\frac{0.15 - x}{0.08}\right) \right] \sum \sigma_R(\tilde{E}), \quad (\text{A2})$$

where the suppression factor in the square bracket represents the threshold $\tilde{E}_{\text{th}} = 0.15 \text{ GeV}$ of $p\gamma$ interactions with $x = \tilde{E}/\text{GeV}$. Moreover, Rachen (1996) found that the cross section in the high energy region ($\tilde{E}_0 > 0.727 \text{ GeV}$) can be

Table A1. Parameters for resonances.

Name	$m_R c^2 / \text{GeV}$	$\bar{\Gamma} / \text{GeV}$	$\sigma_0 / \mu\text{barn}$
$\Delta(1232)$	1.231	0.11	31.125
$N(1440)$	1.44	0.35	1.389
$N(1520)$	1.515	0.11	25.567
$N(1535)$	1.525	0.1	6.948
$N(1650)$	1.675	0.16	2.779
$N(1680)$	1.68	0.125	17.508
$\Delta(1700)$	1.69	0.29	11.116
$\Delta(1905)$	1.895	0.35	1.667
$\Delta(1950)$	1.95	0.3	11.116

fitted by²

$$\sigma_2(\tilde{E}) = \left[1 - \exp\left(\frac{0.727 - x}{0.8}\right) \right] \times (0.067y^{0.081} + 0.125y^{-0.453}) \text{ mbarn.} \quad (\text{A3})$$

where $y = s/\text{GeV}^2$. Subtracting the two components expressed by Eqs. A2 and A3 from the experimental data taken from particle data group (Yao et al. 2006), we find the residuals to the total cross section exhibit a broken power-low behavior, which yields

$$\sigma_3(\tilde{E}) = \left[1 - \exp\left(\frac{0.15 - x}{0.08}\right) \right] \times 0.072x^{-1.6} \left[\left(\frac{0.62}{x}\right)^{20} + 1 \right]^{-0.21} \times \left[\left(\frac{0.46}{x}\right)^{20} + 1 \right]^{0.225} \left[\left(\frac{0.28}{x}\right)^{20} + 1 \right]^{-0.45} \text{ mbarn.} \quad (\text{A4})$$

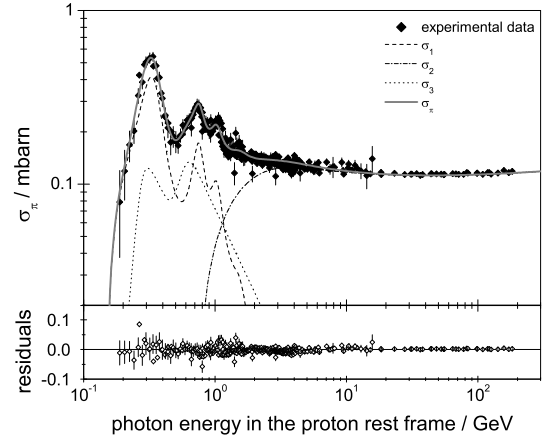
Roughly speaking, the above formula could be related with the direct single-pion production processes. Finally, combining the three components, we can express the total cross section of $p\gamma$ interactions by

$$\sigma_\pi(\tilde{E}) = \begin{cases} \sigma_1 + \sigma_3, & \text{for } 0.15\text{GeV} < \tilde{E}_0 < 0.727\text{GeV}; \\ \sigma_1 + \sigma_2 + \sigma_3, & \text{for } \tilde{E}_0 > 0.727\text{GeV}. \end{cases} \quad (\text{A5})$$

We confront this exponential formula with the experimental data in Fig. A1. It can be seen the fits is good, although the formula can not describe the detailed physics.

REFERENCES

- Asano K., 2005, ApJ, 623, 967
Asano K. & Nagataki S., 2006, ApJ, 640, L9
Blustin A.J., 2007, to appear in Phil. Trans. Roy. Soc. A, Proceedings of the Royal Society Discussion meeting on Gamma-Ray Bursts, September 18-20, arXiv: astr-ph/0701804
Campana S. et al., 2006, Nature, 442, 1008
Chevalier R.A. & Li Z.Y., 2000, ApJ, 536, 195
Cobb B.E., Bailyn C.D., van Dokkum P.G. & Natarajan P., 2006, ApJ, 645, L113
Dai Z.G. & Lu T., 1998, MNRAS, 298, 87
Dai Z.G. & Lu T., 2001, ApJ, 551, 249
Dermer C.D., 2002, ApJ, 574, 65
Dermer C.D. & Atoyan A. 2003, Phys. Rev. Lett., 91, 071102
Fan Y.Z., Piran T. & Xu D., 2006, JCAP, 0609, 013

**Figure A1.** Fits for the total cross section for $p\gamma$ interactions.

- Gupta N. & Zhang B., 2007, Astropart. Phys., 27, 386
Ioka K., Razzaque S., Kobayashi S. & Mészáros P., 2005, ApJ, 633, 1013
Liang E., Zhang B., Virgili F. & Dai Z.G., 2007, ApJ, 662, 1111
Mészáros P. & Rees M.J., 2001, ApJ, 556, L37
Mücke A., Engel R., Rachen J.P. et al., 2000, Comput. Phys. Commun., 124, 290
Murase K., 2007, arXiv: 0707.1140
Murase K. & Nagataki S., 2006a, Phys. Rev. D, 73, 063002
Murase K. & Nagataki S., 2006b, Phys. Rev. Lett., 97, 051101
Murase K., Ioka K., Nagataki S. & Nakamura T., 2006, ApJ, 651, L5
Rachen J.P., 1996, PhD thesis, MPIfR, Bonn, Germany (http://galprop.stanford.edu/na_elibrary.html)
Rachen J.P. & Mészáros P., 1998, Phys. Rev. D, 58, 123005
Ramirez-Ruiz E., Celotti A. & Rees M.J., 2002, MNRAS, 337, 1349
Razzaque S., Mészáros P., & Waxman E., 2004, Phys. Rev. D, 69, 023001
Razzaque S., Mészáros P. & Waxman E., 2006, Phys. Rev. D, 73, 103005
Soderberg A.M. et al., 2006, Nature, 442, 1014
Wang X.Y. & Mészáros P., 2006, ApJ, 643, L95
Waxman E. & Bahcall J., 1997, Phys. Rev. Lett., 78, 2292
Waxman E. & Bahcall J., 1998, Phys. Rev. D, 59, 023002
Waxman E. & Bahcall J., 2000, ApJ, 541, 707
Waxman E., Mészáros P. & Campana S., 2007, ApJ, 667, 351
Yao W.M. et al., 2006, J. Phys. G, 33, 344 (<http://pdg.lbl.gov/2006/hadronic-xsections/hadron.html>)
Zhang W.Q., Woosley S.E. & MacFadyen A.I., 2003, ApJ, 586, 356

² The coefficients here are mildly different from Rachen (1996).